

MULTI-BAND NORMAL ALBEDO MAP OF ASTEROID RYUGU FROM OPPOSITION OBSERVATIONS AT VISIBLE WAVELENGTHS. Y. Yokota^{1,2}, R. Honda², E. Tatsumi^{3,4,5}, D. Domingue⁶, S. E. Schröder⁷, M. Matsuoka¹, S. Sugita⁵, T. Morota^{5,8}, N. Sakatani¹, S. Kameda⁹, T. Kouyama¹⁰, H. Suzuki¹¹, M. Yamada¹², C. Honda¹³, M. Hayakawa¹, K. Yoshioka⁵, Y. Cho⁵, and H. Sawada¹, ¹ISAS/JAXA, (3-1-1 Yoshino-dai, Chuo-ku, Sagamihara, Kanagawa, Japan, yokota@planeta.sci.isas.jaxa.jp). ²Kochi Univ., Japan, ³Instituto de Astrofísica de Canarias, Spain, ⁴Univ. of La Laguna, Spain, ⁵Univ. of Tokyo, Japan, ⁶Planetary Science Institute, USA, ⁷DLR, Germany, ⁸Nagoya Univ., Japan. ⁹Rikkyo Univ., Japan. ¹⁰AIST, Japan, ¹¹Meiji Univ., Japan, ¹²Chiba Inst. Tech, Japan, ¹³Univ. of Aizu, Japan.

Introduction: Asteroid explorer Hayabusa2 observed Cb-type asteroid 162173 Ryugu between June 2018 and November 2019 at a distance below 20km. During this period, the Telescopic Optical Navigation Camera (ONC-T) [1–4] onboard Hayabusa2 observed Ryugu with 7 broadband filters ranging in wavelength from 0.40–0.95 μm . On 8 January 2019, ONC-T observed the asteroid in the opposition geometry from ~ 20 km distance, through one rotation period (7.6 hr). A 7-band image set was obtained every 30° of rotation phase. The local solar phase angle, α , of each pixel ranges from 0.0° to $\sim 1.7^\circ$. Such observations are well suited to derive the normal albedo, defined as the radiance factor (I/F) at $\alpha=0^\circ$ [5]. Here we present the normal albedo map of Ryugu derived from these opposition observations.

Method: The data number of the image pixels are converted to I/F with using the calibration procedures and parameters described in [4]. The observation geometry of each pixel is calculated using the Ryugu shape model [6] produced by the Hayabusa2 shape model team.

Derivation of phase function. The data was binned every 1° in incidence and emission angle, and every 0.1° in phase angle. We excluded data at $i>30^\circ$ and $e>30^\circ$ from fitting. Additionally, to account for the effect of the solar disk size, data within the phase angle range 0.0 – 0.2° were omitted from the fitting. Then, we fit a line to the data set using

$$r_{\text{obs}}(\lambda, \alpha) = a_{0\lambda} + a_{1\lambda} \alpha, \quad (1)$$

where r is I/F for wavelength λ , and $a_{0\lambda}$ and $a_{1\lambda}$ are the fitting parameters. These parameters (Table 1) can be used for photometric correction to obtain the normal albedo using

$$r_{\text{corr.}}(\lambda, 0) = r_{\text{obs.}}(\lambda, \alpha) \frac{a_{0\lambda}}{a_{0\lambda} + a_{1\lambda} \alpha}. \quad (2)$$

Fig. 1 shows the data set for a single ONC band and the fitted line. The equations (1) and (2) do not account for the effects of incidence angle i and emission angle e . We checked the remaining dependency on i and e using large i and e data up to 70° . We found that the dependency is very small ($< \sim 1\%$ of the brightness) over this phase angle range. Such minor dependency

on i and e at near phase angle zero is consistent with the previous studies of other asteroids [7–9]. We decided that additional correction for i and e was not necessary.

Mapping. We assume that the phase curve shape (a straight line for this case) of each band is approximately the same for phase angles $< 1.7^\circ$ for all Ryugu’s surface. Each pixel’s I/F from the 8-Jan-2019 opposition images was converted to normal albedo $r(\lambda, 0)$ using eq. (2). Finally, we projected the $r(\lambda, 0)$ values over the complete rotation set of images to create a mosaic map for each band. The smallest emission angle data is selected for the areas where multiple images are overlapped.

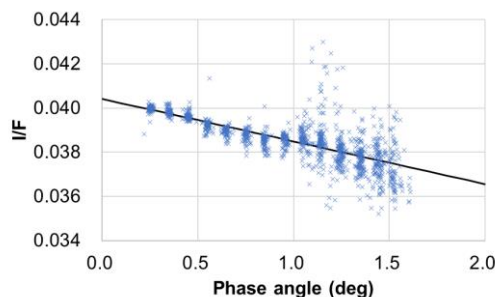


Fig. 1. Phase curve data set (v-band, $0.55 \mu\text{m}$) at near opposition. Black curve is a fitted line.

Results and discussion: Fig. 2 shows the v-band normal albedo map in simple cylindrical projection. Since the observed brightness at the opposition condition is less affected by shadows or topographic undulation than other geometries, the derived map successfully shows the albedo distribution under minimal noise conditions.

The color study [e.g. 1, 6, 10, 11] of Ryugu reported that the spectral slope from b-band ($0.48 \mu\text{m}$) to x-band ($0.86 \mu\text{m}$) exhibits the greatest regional variation on Ryugu. Currently, we found that the normal albedo is well correlated with the b-x spectral slope. Fig. 3 is a false color map made from the normal albedo at ul-, b-, and x-band (0.40 , 0.48 , and $0.86 \mu\text{m}$). Fig. 4 shows a clear correlation between the b-band normal albedo and b/x ratio (simple substitution of the

spectral slope), suggesting that bluer terrain is brighter. However, further study is necessary to interpret this relationship.

Acknowledgment: We thank the entire Hayabusa2 team to achieve the observation and analysis. This study was supported by Japan Society for the Promotion of Science (JSPS) Core-to-Core Program "International Network of Planetary Sciences", NASA's Hayabusa2 participating scientist program (grant number NNX16AL34G), and NASA's Solar System Exploration Research Virtual Institute 2016 (SSERV16) Cooperative Agreement (NNH16ZDA001N) for TREX (Toolbox for Research and Exploration).

References: [1] Sugita S. et al. (2019) *Science* 10.1126/science.aaw0422. [2] Kameda S. et al. (2017) *SSR* 208, 17–31. [3] Suzuki H. et al. (2018) *Icarus* 300, 341–359. [4] Tatsumi E. et al. (2019) *Icarus* 325, 153–195. [5] Li J.-Y., et al. (2015) *Asteroids IV*, University of Arizona Press, 129–

150. [6] Watanabe S. et al. (2019) *Science* 364, 268–272. [7] Schröder S. E. et al. (2013) *PSS* 85, 198–213. [8] Hasselmann P. H. et al. (2016) *Icarus* 267, 135–153. [9] Schröder S. E. et al. (2017) *Icarus* 288, 201–225 [10] Morota T. et al. (2020) (submitted). [11] Tatsumi E. et al. (2020) (in preparation).

Table 1. Derived parameters

Band	Wavelength (nm)	a_0	a_1
ul	397.5	0.04373	-0.002289
b	479.8	0.04051	-0.001875
v	548.9	0.04041	-0.001927
Na	589.9	0.04051	-0.001915
w	700.1	0.04020	-0.002004
x	857.3	0.04095	-0.002189
p	945.1	0.03973	-0.002185

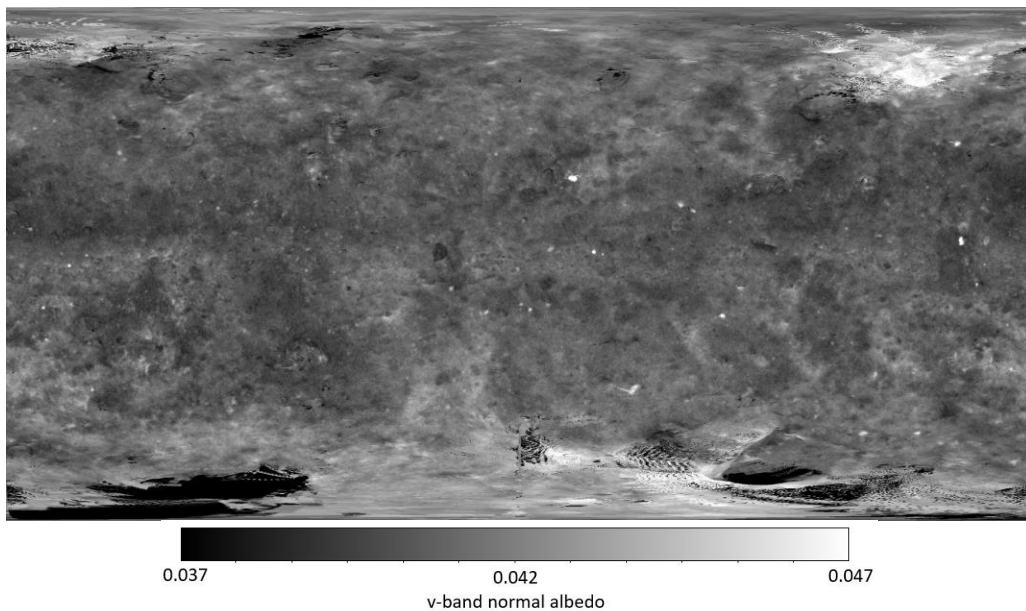


Fig. 2. Normal albedo (I/F at phase angle zero) map of Ryugu at v-band ($0.55 \mu\text{m}$). Black indicates the un-observed area.

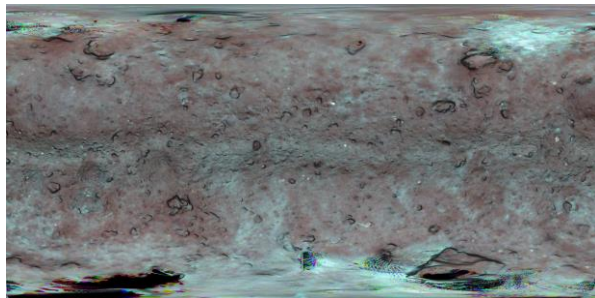


Fig. 3. False color map made from the normal albedo at ul-, b-, and x-band ($0.40, 0.48, \text{ and } 0.86 \mu\text{m}$). RGB channels are assigned as Blue=ul, Green=b, and Red=x. Shaded relief of topography [6] is overlaid on the map.

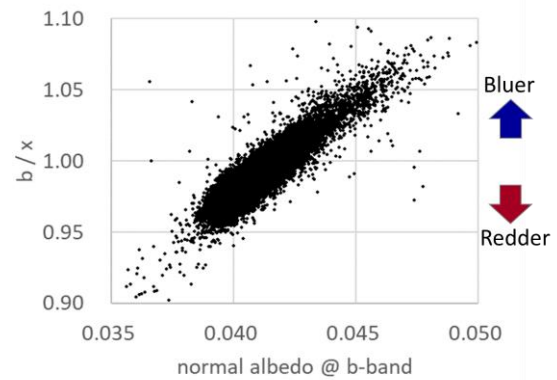


Fig. 4. Normal albedo ratio of b-band ($0.48 \mu\text{m}$) / x-band ($0.86 \mu\text{m}$) is shown as a function of b-band normal albedo. Global data of $\sim 8 \times 8 \text{ m}$ (1 deg at equator) size bin is plotted.